

Proteolytic Activation of the Human Epithelial Sodium Channel by Trypsin IV and Trypsin I Involves Distinct Cleavage Sites*

Received for publication, December 24, 2013, and in revised form, May 10, 2014. Published, JBC Papers in Press, May 19, 2014, DOI 10.1074/jbc.M113.538470

Silke Haerteis[‡], Annabel Krappitz[‡], Matteus Krappitz[‡], Jane E. Murphy[§], Marko Bertog[‡], Bettina Krueger[‡], Regina Nacken[‡], Hyunjae Chung[¶], Morley D. Hollenberg[¶], Wolfgang Knecht[¶], Nigel W. Bunnett^{**††}, and Christoph Korbmacher^{‡1}

From the [‡]Institut für Zelluläre und Molekulare Physiologie, Friedrich-Alexander-Universität Erlangen-Nürnberg (FAU), Waldstrasse 6, 91054 Erlangen, Germany, the [§]UCSF Center for the Neurobiology of Digestive Diseases, Department of Surgery, University of California, San Francisco, California, the [¶]Department of Physiology and Pharmacology, University of Calgary, Calgary, Alberta T2N 4N1, Canada, ^{||}Bioscience, CVGI iMed, AstraZeneca Research and Development, 43181 Mölndal, Sweden, the ^{**}Monash Institute of Pharmaceutical Sciences, 381 Royal Parade, Parkville, Victoria 3052, Australia, and the ^{††}Department of Pharmacology, University of Melbourne, Melbourne, Victoria 3010, Australia

Background: Proteolysis is required for ENaC activity, but the proteases activating ENaC in epithelial tissues are unknown.

Results: Human trypsin IV and trypsin I activate ENaC by cleavage at distinct sites in the channel's γ -subunit.

Conclusion: Cleavage at distinct sites may provide a mechanism for differential ENaC regulation by tissue-specific proteases.

Significance: ENaC activation by trypsin IV may contribute to ENaC regulation *in vivo*.

Proteolytic activation is a unique feature of the epithelial sodium channel (ENaC). However, the underlying molecular mechanisms and the physiologically relevant proteases remain to be identified. The serine protease trypsin I can activate ENaC *in vitro* but is unlikely to be the physiologically relevant activating protease in ENaC-expressing tissues *in vivo*. Herein, we investigated whether human trypsin IV, a form of trypsin that is co-expressed in several extrapancreatic epithelial cells with ENaC, can activate human ENaC. In *Xenopus laevis* oocytes, we monitored proteolytic activation of ENaC currents and the appearance of γ ENaC cleavage products at the cell surface. We demonstrated that trypsin IV and trypsin I can stimulate ENaC heterologously expressed in oocytes. ENaC cleavage and activation by trypsin IV but not by trypsin I required a critical cleavage site (Lys-189) in the extracellular domain of the γ -subunit. In contrast, channel activation by trypsin I was prevented by mutating three putative cleavage sites (Lys-168, Lys-170, and Arg-172) in addition to mutating previously described prostatic (RKRR¹⁷⁸), plasmin (Lys-189), and neutrophil elastase (Val-182 and Val-193) sites. Moreover, we found that trypsin IV is expressed in human renal epithelial cells and can increase ENaC-mediated sodium transport in cultured human airway

epithelial cells. Thus, trypsin IV may regulate ENaC function in epithelial tissues. Our results show, for the first time, that trypsin IV can stimulate ENaC and that trypsin IV and trypsin I activate ENaC by cleavage at distinct sites. The presence of distinct cleavage sites may be important for ENaC regulation by tissue-specific proteases.

The epithelial sodium channel (ENaC)² is the rate-limiting step for transepithelial sodium transport in several sodium-absorbing tissues, including the distal colon, the aldosterone-sensitive distal nephron, and respiratory epithelia (1, 2). ENaC is a member of the ENaC/degenerin family of non-voltage-gated ion channels, which also includes the acid-sensing ion channel ASIC1. The available crystal structure of chicken ASIC1 (3, 4) and studies of ENaC by atomic force microscopy (5) suggest that ENaC is a heterotrimer composed of three homologous subunits (α , β , and γ). Each subunit of ENaC contains two transmembrane domains, a large extracellular domain, and short intracellular amino and carboxyl termini.

A unique feature of ENaC regulation is that proteolytic processing is critical for channel activation (6, 7). However, the precise molecular mechanisms of proteolytic channel activation and the proteases involved remain to be elucidated. Proteolytic cleavage occurs at specific residues within the extracellular domains of the α - and γ -subunit of ENaC. Proteolytic cleavage at three putative furin sites (two in α ENaC and one in γ ENaC) probably occurs before the channel reaches the plasma

* This work was supported, in whole or in part, by National Institutes of Health Grants DK43207 and DK57840 (to N. W. B.). This work was also supported by grants from the Interdisziplinäres Zentrum für Klinische Forschung (IZKF) (to S. H. and M. K.) and the Erlanger Leistungsbezogene Anschubfinanzierung und Nachwuchsfoerderung (ELAN) program of the Friedrich-Alexander-Universität Erlangen-Nürnberg (FAU) (to S. H.), by National Health and Medical Research Council Grants 63303, 1049682, 1031886 and Monash University (to N. W. B.), and by grants from Prostate Cancer Canada and the Canadian Institutes of Health Research (CIHR) (to M. D. H.). The Bio-Organic Biomedical Mass Spectrometry Resource at the University of California, San Francisco, is supported by the Biomedical Research Technology Program of the National Institutes of Health, NCR, Grants P41RR001614 and 1S1ORR014606.

¹ To whom correspondence should be addressed. Tel.: 49-9131-8522300; Fax: 49-9131-8522770; E-mail: christoph.korbmacher@fau.de.

² The abbreviations used are: ENaC, epithelial sodium channel; $\Delta I_{\text{amiloride}}$, amiloride-sensitive current; I_{SC} , short circuit current; SBTI, soybean trypsin inhibitor; cRNA, complementary RNA; HPTC, human proximal tubular cell; RKRR178AAA, mutation of RKRR¹⁷⁸ to AAAA; FF174AA, mutation of FF¹⁷⁴ to AA.

Trypsin IV Cleavage and Activation of ENaC

membrane. A second cleavage event in γ ENaC is required as the critical final step in proteolytic channel activation and probably happens at the plasma membrane, where γ ENaC is cleaved by membrane-bound or extracellular proteases in a region distal to the furin site. This concept is supported by the finding that the time course of proteolytic activation of ENaC-mediated whole-cell currents correlates with the appearance of a ~ 67 kDa γ ENaC cleavage product at the cell surface (8).

The proteases that activate ENaC under physiological and pathophysiological conditions have not been clearly identified and may differ between tissues. Putative cleavage sites in γ ENaC have been described for the serine proteases prostatic (9), plasmin (8, 10), elastase (11), kallikrein (12), and chymotrypsin (8). In contrast, the sites at which trypsins cleave and activate ENaC have not yet been identified. The prototypical serine proteases trypsin I and chymotrypsin are commonly used as experimental tools to achieve maximal proteolytic ENaC activation (13, 14). There is evidence that trypsin I is expressed in epithelial cells (15) and can be detected in human urine (16) (Human Urine, PeptideAtlas, June 2010). However, it is unclear whether trypsin I plays a physiological role for ENaC activation *in vivo* because trypsinogen I is mainly found in the exocrine pancreas.

Trypsinogens are encoded by a diverse gene family with considerable interspecies variability. In the human genome, three serine protease (*PRSS*) genes that encode trypsinogens have been identified: *PRSS1*, *PRSS2*, and *PRSS3*. The *PRSS1* and *PRSS2* genes are located on chromosome 7q34 and encode trypsinogen I and trypsinogen II, respectively. The *PRSS3* gene, which is localized on chromosome 9p11.2, encodes mesotrypsinogen and a splice variant referred to as trypsinogen IV (17–19). After cleavage/activation by enteropeptidase (enterokinase), both precursor proteins result in the same active protease, which is referred to as mesotrypsin or trypsin IV. Trypsinogen IV is expressed by neurons and astrocytes of human brain and spinal cord and is widely expressed in extrapancreatic epithelial cells, including those of the airway, prostate, and colon that are known to express ENaC (15, 18, 20, 21, 34). In contrast to trypsin I and II, which are inhibited by endogenous polypeptide inhibitors, trypsin IV is resistant to many endogenous inhibitors. Trypsin IV also degrades polypeptide inhibitors. Thus, released trypsin IV may remain active for prolonged periods. Indeed, trypsin IV is a candidate protease for regulating inflammation and pain (22–24). Trypsin IV also contributes to metastasis of prostate cancer and may be a therapeutic target (25, 26).

The inappropriate activation of ENaC by locally generated proteases may contribute to several patho-physiological conditions. For example, tubular fluid plasmin, which can be generated from filtered plasminogen by tubular urokinase, can activate ENaC in the kidney and thereby cause renal sodium retention in nephrotic syndrome (27). Similarly, proteolytic ENaC activation in the colon may minimize sodium and fluid loss in early stages of inflammation (28). The widespread co-expression of trypsin IV and ENaC in epithelial tissues and the appreciation that trypsin IV may be generated during disease, led us to examine whether trypsin IV can activate ENaC.

Our objective was to investigate proteolytic ENaC activation by trypsin IV and to identify functionally relevant cleavage sites for trypsin IV and trypsin I in the γ -subunit of ENaC. Our study provides new insights into the mechanisms of proteolytic ENaC activation by trypsin I and trypsin IV.

EXPERIMENTAL PROCEDURES

Materials—Amiloride hydrochloride and soybean trypsin inhibitor (SBTI) was obtained from Sigma. The solutions used were as follows: OR2 (82.5 mM NaCl, 2 mM KCl, 1 mM MgCl₂, 5 mM HEPES, pH 7.4, with NaOH), ND96 (96 mM NaCl, 2 mM KCl, 1.8 mM CaCl₂, 1 mM MgCl₂, 5 mM HEPES, pH 7.4, with Tris), and a low Na⁺-containing solution for oocyte incubation (87 mM NMDG-Cl, 9 mM NaCl, 2 mM KCl, 1.8 mM CaCl₂, 1 mM MgCl₂, 5 mM HEPES, pH 7.4, with Tris). To prevent bacterial overgrowth, solutions for oocyte incubation were supplemented with 100 units/ml penicillin and 100 μ g/ml streptomycin. The serine protease inhibitor melagatran has been described (23).

Proteases—Recombinant human trypsinogen IV was expressed, purified, and activated to generate trypsin IV as described (22). The specific activity of trypsin IV was determined to be 74 units/mg using *N*-(*p*-Tosyl)-Gly-Pro-Arg *p*-nitroanilide acetate salt as substrate (22). Bovine trypsin I and α -chymotrypsin II were from Sigma.

ENaC Fragments—A 23-mer γ ENaC peptide was synthesized and purified by the Peptide Synthesis Core Facility (University of Calgary, Canada) (purity >95%). The peptide sequence (¹⁷⁶TGRKRKVGGSIIHKASNVMIHIES¹⁹⁸) (11, 29) corresponds to the amino acid sequence from Thr-176 to Ser-198 of the extracellular domain of γ ENaC thought to be critical for proteolytic channel activation.

Plasmids—Full-length cDNAs for human wild-type α -, β -, and γ ENaC were kindly provided by Harry Cuppens (Leuven, Belgium). They were subcloned into pcDNA3.1 vector, and linearized plasmids were used as templates for cRNA synthesis (mMessage mMachine, Ambion, Austin, TX) using T7 as promoter as described previously (30, 31). The γ ENaC mutants γ_{K189A} (8), $\gamma_{K168A,K170A,R172A}$, $\gamma_{RKRK178AAAA,V182G,V193G,K189A}$ and $\gamma_{K168A,K170A,R172A,RKRK178AAAA,V182G,V193G,K189A}$ were generated by site-directed mutagenesis (QuikChange[®] site-directed mutagenesis kit, Stratagene, Amsterdam, Netherlands) and sequences were confirmed (LGC Genomics, Berlin, Germany). To minimize the risk of expression artifacts that may arise from differences in cRNA quality, cRNAs for wild-type and mutant ENaC were synthesized in parallel, and the experiments were performed using at least two different batches of complementary RNA.

Isolation of Oocytes and Injection of cRNA—Oocytes were obtained from adult *Xenopus laevis* in accordance with the principles of German legislation, with approval by the animal welfare officer for the Friedrich-Alexander-University Erlangen-Nürnberg (FAU) and under the governance of the state veterinary health inspectorate (permit 621-2531.32-05/02). Animals were anesthetized in 0.2% MS222 (ethyl 3-aminobenzoate methanesulfonate salt). Ovarian lobes were obtained by partial ovariectomy, and oocytes were isolated by enzymatic digestion at 19 °C for 3–4 h with 600–700 units/ml collagenase CLS II (Biochrom, Berlin, Germany) dissolved in OR2 solution.

Defolliculated stage V-VI oocytes were injected (Nanoject II automatic injector, Drummond, Broomall, PA) with 0.2 ng of cRNA/subunit of ENaC. The cRNAs were dissolved in RNase-free water, and the total volume injected was 46 nl. Injected oocytes were stored at 19 °C in a low Na⁺-containing solution.

Two-electrode Voltage Clamp—Oocytes were routinely studied 2 days after injection using the two-electrode voltage clamp technique as described previously (8, 29–31). Individual oocytes were placed in a small experimental chamber and constantly superfused (2–3 ml/min) at room temperature with ND96 supplemented with amiloride (2 μM). Bath solution exchanges were controlled by a magnetic valve system (ALA BPS-8) in combination with a TIB14 interface (both HEKA, Lambrecht, Germany). Voltage clamp experiments were performed using an OC-725C amplifier (Warner Instruments Corp., Hamden, CT) interfaced via a LIH-1600 (HEKA) to a PC with PULSE 8.67 software (HEKA) for data acquisition and analysis. Oocytes were clamped at a holding potential of –60 mV. Downward current deflections in the current traces correspond to inward currents (*i.e.* movement of positive charge from the extracellular side into the cell). Amiloride-sensitive whole-cell currents (ΔI_{ami}) were determined by washing out amiloride with amiloride-free ND96 and subtracting the whole-cell currents measured in the presence of amiloride from the corresponding whole-cell currents recorded in the absence of amiloride. For the determination of the effect of trypsin I or chymotrypsin, continuous whole-cell current measurements were performed, and ΔI_{ami} was measured again after superfusing the oocyte with the protease. For the determination of the stimulatory effect of trypsin IV, ΔI_{ami} was determined twice in a single oocyte (*i.e.* before and after exposure to the protease). To recover from the first measurement of ΔI_{ami} , the oocyte was placed for 5 min in ND96. Subsequently, the oocyte was transferred to 100 μl of test solution (protease-supplemented ND96 or protease-free ND96 solution as control) and was incubated for 30 min before ΔI_{ami} was determined for a second time.

Detection of γ ENaC Cleavage Products at the Cell Surface—Biotinylation experiments were performed as described previously (8, 29), using 30 oocytes/group. All biotinylation steps were performed at 4 °C. Oocytes were preincubated for 30 min either in ND96 solution or in ND96 solution containing proteases. After washing the oocytes three times with ND96 solution, they were incubated in the biotinylation buffer (10 mM triethanolamine, 150 mM NaCl, 2 mM CaCl₂, and 1 mg/ml EZ-link sulfo-NHS-SS-Biotin (Thermo Fisher Scientific, Schwerte, Germany), pH 9.5) for 15 min with gentle agitation. The biotinylation reaction was stopped by washing the oocytes twice for 5 min with quench buffer (192 mM glycine and 25 mM Tris-Cl, pH 7.5). Subsequently, the oocytes were lysed by passing them through a 27-gauge needle in lysis buffer (500 mM NaCl, 5 mM EDTA, and 50 mM Tris-Cl, pH 7.4) supplemented with protease inhibitor mixture tablets (Complete Mini EDTA-free; Roche Applied Science) according to the manufacturer's instructions. The lysates were centrifuged for 10 min at 1,500 × *g*. Supernatants were incubated with 0.5% Triton X-100 and 0.5% Igepal CA-630 for 20 min on ice. Biotinylated proteins were precipitated with 100 μl of Immunopure-immobilized NeutrAvidin-agarose (Thermo Fisher Scientific) washed with lysis buffer. After overnight incubation at 4 °C with overhead rotation,

the tubes were centrifuged for 3 min at 1,500 × *g*. Supernatants were removed, and beads were washed three times with lysis buffer. 100 μl of 2× SDS-PAGE sample buffer (Rotiload 1, Roth, Karlsruhe, Germany) was added to the beads. Samples were boiled for 5 min at 95 °C and centrifuged for 3 min at 20,000 × *g* before loading the supernatants onto a 10% SDS-polyacrylamide gel. To detect γ ENaC cleavage fragments, we used a subunit-specific antibody against human γ ENaC at a dilution of 1:5,000 (8, 29, 30, 32). Horseradish peroxidase-labeled secondary goat anti-rabbit antibody (Santa Cruz Biotechnology, Inc.) was used at a dilution of 1:50,000. Chemiluminescence signals were detected using Super-Signal West Femto chemiluminescent substrate (Thermo Fisher Scientific).

High-performance Liquid Chromatography (HPLC) and Matrix-assisted Laser Desorption Ionization-Time-of-flight (MALDI-TOF) Analysis—The 23-mer γ ENaC peptide (500 μM) was incubated with 50 μg/ml trypsin IV in 50 mM Tris-HCl, pH 7.4, for 30 min at 37 °C. Products were separated by reversed-phase HPLC and identified using MALDI-TOF. Mass spectrometry data were provided by the Bio-Organic Biomedical Mass Spectrometry Resource at the University of California, San Francisco (A. L. Burlingame, Director).

Reverse Transcription PCR (RT-PCR)—Human kidney tissues were collected from patients undergoing nephrectomy with the approval of the ethics board at the University of Calgary and Alberta Health Services in Canada. We established human proximal tubular cell (HPTC) cultures from disease-free dissected nephrectomy samples, as described previously (33). In summary, normal cortex segments of the nephrectomy samples were finely dissected, minced, and digested with collagenase IV (1.5 mg/ml) at 37 °C for 60 min. Samples were passed through a 70-μm mesh and were centrifuged, rinsed, and plated on plastic culture plates at 37 °C for 90 min in K1 culture medium (DMEM/F-12 containing 10% fetal bovine serum, 1% penicillin-streptomycin, prostaglandin E1 (125 ng/ml), epidermal growth factor (25 ng/ml), L-thyroxine (1.8 μg/ml), hydrocortisone (3.38 ng/ml), insulin (5 μg/ml), transferrin (5 μg/ml), and sodium selenite (5 ng/ml); all reagents were purchased from Sigma). Nonadherent cells were replated onto collagen IV-coated cell culture plate.

An RT-PCR was performed to assess expression of trypsinogen IV at the messenger RNA level. Total RNA from human kidney tissue or cultured HPTCs or prostate cancer-derived human epithelial cells (PC3, CRL-1435TM; ATCC (Manassas, VA)) was extracted using an RNAeasy kit (Qiagen) and transcribed to cDNA using Moloney murine leukemia virus transcriptase (Invitrogen) according to the manufacturer's protocol. Semiquantitative PCR was performed using *Taq* DNA polymerase (Qiagen Inc., Canada) as per the manufacturer's protocol. PCR primers were selected that are specific for human trypsinogen IV (34): forward primer, 5'-GGGCCTG-GAGCTGCACCCGCTTCTG-3'; reverse primer, 5'-CAGC-CGGAGATGAGGCATC-3'. The expected PCR product size is 474 bp. Thermal cycling was performed in a PTC-100 programmable thermocontroller using the following cycle parameters: denaturation at 94 °C for 30 s, annealing at 62 °C for 30 s, and elongation at 72 °C for 30 s. The number of cycles was 36, and the PCR products were electrophoresed on a 1.5% agarose

Trypsin IV Cleavage and Activation of ENaC

gel containing SYBR safe. DNA was prepared from bands of the agarose gel with the QIAquick gel extraction kit (Qiagen) according to the manufacturer's protocol. The sequence of the purified product was confirmed by the sequencing services at the University of Calgary.

H441 Cell Culture and Transepithelial Measurements—The human H441 lung epithelial cell line (HTB-174TM) was obtained from ATCC. Cells were used at passage 64–66 and cultured as described previously (35). Cells were maintained in a 5% CO₂ atmosphere at 37 °C in H441 growth medium consisting of RPMI 1640 (Rosewell Park Memorial Institute, Biochrom) medium supplemented with 10% fetal bovine serum, L-glutamine (2 mM), apotransferrin (5 µg/ml), insulin (5 µg/ml), sodium selenite (10 nM), sodium pyruvate (1 mM), 100 units/ml penicillin, and 100 µg/ml streptomycin. For transepithelial measurements, cells were cultured on permeable support (Millicell PCF membrane inserts, Merck-Millipore, Schwalbach, Germany) in H441 growth medium. At day 9 after seeding, this medium was replaced in the basolateral compartment by a differentiation medium (RPMI 1640 supplemented with 4% charcoal-stripped serum, triiodothyronine (1 nM), dexamethasone (200 nM), apotransferrin (5 µg/ml), insulin (5 µg/ml), sodium selenite (10 nM)). The apical side of the epithelial monolayer was kept at an air-liquid interface. After 4–5 days at the air-liquid interface, the monolayers were transferred into Ussing chambers to measure the equivalent short circuit current (I_{SC}) essentially as described previously (36). To record the transepithelial voltage and resistance, a Ringer's solution (117 mM NaCl, 25 mM NaHCO₃, 4.7 mM KCl, 1.2 mM MgSO₄, 1.2 mM KH₂PO₄, 2.5 mM CaCl₂, 11 mM D-glucose, equilibrated to pH 7.4 with a 5% CO₂ atmosphere) was added to the apical compartment. To minimize ENaC activation by endogenous proteases (27, 29, 37) prior to the application of trypsin IV, the H441 cells were exposed for 90 min to SBTI (10 µg/ml) in the apical bath and to the furin/convertase inhibitor decanoyl-Arg-Val-Lys-Arg-chloromethyl ketone (Merck-Millipore), which was added to the basolateral bath solution. A 10 mM stock solution of decanoyl-Arg-Val-Lys-Arg-chloromethyl ketone was prepared in DMSO, and the final concentration used was 40 µM.

Statistical Analysis—Data are presented as mean ± S.E. N indicates the number of different batches of oocytes, and n is the number of individual oocytes studied. Statistical significance was assessed by the appropriate version of Student's t test with GraphPad Prism version 5.04 (GraphPad Software).

RESULTS

Trypsin IV Stimulates ENaC Currents in *X. laevis* Oocytes Expressing Human ENaC—To investigate whether trypsin IV activates ENaC, we determined amiloride-sensitive whole-cell currents (ΔI_{ami}) in individual ENaC-expressing oocytes before and after 30-min incubation of the oocytes with trypsin IV (10 µg/ml). Control oocytes were incubated with the prototypical serine protease trypsin I (2 µg/ml) for maximal ENaC activation or were incubated in protease-free solution. Fig. 1 (A–C) shows six representative whole-cell current traces from one batch of oocytes. Currents in individual oocytes were measured twice: before and after a 30-min exposure to protease-free solution (Fig. 1A), trypsin I (Fig. 1B), or trypsin IV (Fig. 1C). In Fig. 1D, ΔI_{ami} values measured

in the same oocyte before and after a 30-min incubation period were connected by a line. Exposure to trypsin IV or trypsin I increased ΔI_{ami} in each oocyte measured. In contrast, a 30-min incubation of oocytes in protease-free solution had no stimulatory effect on ENaC currents (Fig. 1D). In these oocytes, ENaC currents remained stable or slightly declined, consistent with the well known phenomenon of spontaneous channel “rundown” (38). On average, exposure to trypsin IV and trypsin I increased ΔI_{ami} by 2.5- and 4.8-fold, respectively (Fig. 1E). Thus, human trypsin IV can activate ENaC currents in human $\alpha\beta\gamma$ ENaC-expressing oocytes.

The Serine Protease Inhibitor Melagatran Prevents Trypsin IV and Trypsin I Activation of ENaC—To confirm that the observed ENaC activation is caused by the proteolytic activity of trypsin IV and not by a contaminant, we examined the effect of the serine protease inhibitor melagatran, which inhibits both trypsin IV and trypsin I (23). ΔI_{ami} was measured before and after 30-min incubation of oocytes in solutions containing trypsin I (2 µg/ml), trypsin IV (10 µg/ml), melagatran (10 µM), trypsin I plus melagatran, or trypsin IV plus melagatran. Control oocytes were incubated in protease-free solution. To ensure an optimal inhibitory effect of melagatran, trypsin I or IV was preincubated with melagatran for 20 min at 37 °C before incubation with oocytes. These experiments demonstrated that melagatran abolished trypsin I- and trypsin IV-stimulated ENaC activation (Fig. 2). Thus, proteolytic activity of trypsin I and trypsin IV is needed for channel activation.

The Polypeptide Inhibitor SBTI Prevents Activation of ENaC by Trypsin I but Not Trypsin IV—In order to distinguish between a stimulatory action of trypsin I and trypsin IV, we used the polypeptide inhibitor SBTI. SBTI forms a stable, enzymatically inactive complex with trypsin I and also inhibits other proteases, including chymotrypsin, plasmin, and plasma kallikreins. In contrast, trypsin IV is resistant to polypeptide trypsin inhibitors, such as SBTI, which it also degrades (18, 19, 22, 34). Therefore, SBTI should inhibit proteolytic activation of ENaC by trypsin I but not by trypsin IV. To test this possibility, ΔI_{ami} was measured before and after 30-min incubation of oocytes in solutions containing trypsin I, trypsin IV, trypsin I plus SBTI, or trypsin IV plus SBTI. Control oocytes were incubated in protease-free solution. To ensure an optimal inhibitory effect of SBTI, trypsin I and trypsin IV were preincubated with SBTI for 20 min before exposure to oocytes. As expected, SBTI inhibited trypsin I-activation of ENaC in a concentration-dependent manner. Using a trypsin I/SBTI ratio of 1:1 significantly reduced the stimulatory effect of trypsin I on ΔI_{ami} . Using a 1:3.2 or 1:10 ratio (trypsin I/SBTI) almost completely abolished the stimulation. In contrast, in experiments with a trypsin IV/SBTI ratio of 1:1 or 1:3.2, the stimulatory effect of trypsin IV on ENaC was not diminished by SBTI (Fig. 3). These findings are consistent with the known resistance of trypsin IV to SBTI.

Trypsin IV Cleaves within the Extracellular Domain of Human γ ENaC—To identify putative cleavage sites for trypsin IV, a 23-mer γ ENaC peptide (¹⁷⁶TGRKRKVGGSIIHKAS-NVMHIES¹⁹⁸) was synthesized that corresponded to a region

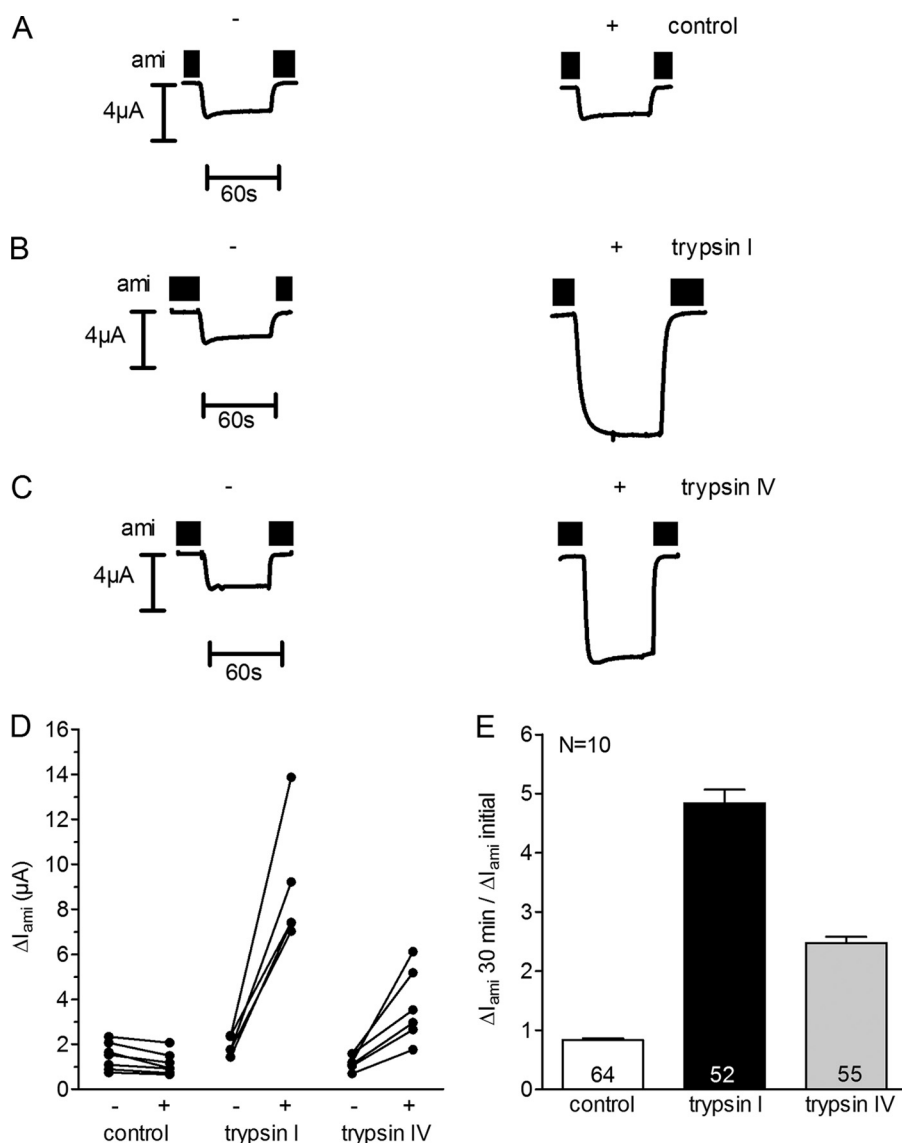


FIGURE 1. Trypsin IV stimulates ENaC currents in *X. laevis* oocytes expressing human ENaC. Oocytes expressing human $\alpha\beta\gamma$ ENaC were preincubated for 30 min in protease-free solution (control) or in solution containing either trypsin I (2 $\mu\text{g}/\text{ml}$) or trypsin IV (10 $\mu\text{g}/\text{ml}$). Amiloride-sensitive whole-cell currents (ΔI_{ami}) were determined before (–) and after (+) incubation. A–C, six representative whole-cell current traces from one batch of oocytes are shown. Amiloride (*ami*) was present in the bath solution to specifically inhibit ENaC, as indicated by black bars. D, individual ΔI_{ami} values measured in one batch of oocytes. Data points obtained from an individual oocyte are connected by a line. E, summary of similar experiments as shown in D performed in 10 different batches of oocytes ($n = 10$). Columns represent the relative stimulatory effect of the incubation on ΔI_{ami} calculated as the ratio of ΔI_{ami} measured after 30-min incubation ($\Delta I_{ami} 30 \text{ min}$) to the initial ΔI_{ami} ($\Delta I_{ami} \text{ initial}$) measured before incubation. The numbers inside the columns indicate the number of individual oocytes measured. Error bars, S.E.

in the extracellular domain of γ ENaC that contains cleavage sites known to be relevant for proteolytic channel activation (8, 11, 29) (Fig. 4A). The 23-mer γ ENaC peptide was incubated with trypsin IV (50 $\mu\text{g}/\text{ml}$) for 30 min, and degradation was assessed using HPLC and MALDI-TOF mass spectrometry (Fig. 4B). Trypsin IV degraded the γ ENaC fragment and generated two products that were identified by mass spectrometry and are consistent with hydrolysis at $\gamma\text{K}^{189} \downarrow \text{A}^{190}$.

Mutation of $\gamma\text{K}189\text{A}$ Suppresses ENaC Activation by Trypsin IV, Not Trypsin I—Trypsin IV is known to target the amino acids lysine or arginine preferentially. Our MADLI-TOF data suggest that trypsin IV cleaves at $\gamma\text{Lys-189}$ (Fig. 4B). Recently, we have shown that the Lys-189 site is also the preferential cleavage site for plasmin (8). To investigate the functional relevance of this site for channel activation by trypsin IV, we com-

pared the effect of trypsin I and trypsin IV on ENaC currents of oocytes expressing wild-type ENaC or the $\alpha\beta\gamma_{\text{K}189\text{A}}$ mutant channel (8). We measured ΔI_{ami} in individual oocytes before and after 30-min exposure to protease-free solution, trypsin I (2 $\mu\text{g}/\text{ml}$), or trypsin IV (10 $\mu\text{g}/\text{ml}$). Baseline ΔI_{ami} in wild-type ENaC-expressing oocytes was similar to that in oocytes expressing the $\alpha\beta\gamma_{\text{K}189\text{A}}$ mutant channel (Fig. 5A). As shown in Fig. 5B, trypsin I stimulated ΔI_{ami} of wild-type and mutant ENaC-expressing oocytes to a similar extent (5.0-fold). In contrast, the stimulatory response to trypsin IV was significantly reduced in oocytes expressing the mutant channel compared with oocytes expressing wild-type ENaC (Fig. 5B). Our results show that mutating lysine 189 to alanine inhibits the stimulatory effect of trypsin IV on ENaC, whereas the stimulatory response to trypsin I is fully preserved. Thus,

Trypsin IV Cleavage and Activation of ENaC

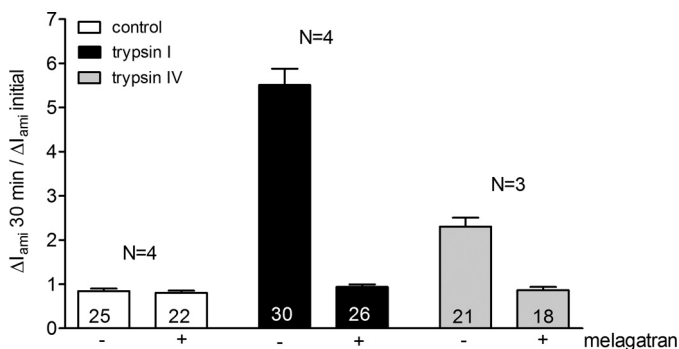


FIGURE 2. The serine protease inhibitor melagatran prevents trypsin IV and trypsin I activation of ENaC. Oocytes expressing $\alpha\beta\gamma$ ENaC were incubated for 30 min in protease-free solution (control), in trypsin I (2 μ g/ml), in trypsin IV (10 μ g/ml), in melagatran (10 μ M), in trypsin I (2 μ g/ml) plus melagatran (10 μ M), or in trypsin IV (10 μ g/ml) plus melagatran (10 μ M). Amiloride-sensitive whole-cell currents (ΔI_{ami}) were determined before and after incubation. Columns represent the relative effect of the incubation on ΔI_{ami} calculated as the ratio of ΔI_{ami} measured after 30-min incubation (ΔI_{ami} 30 min) to the initial ΔI_{ami} (ΔI_{ami} initial) measured before incubation. The numbers inside the columns indicate the number of individual oocytes measured. N, number of different batches of oocytes used for the experiments. Error bars, S.E.

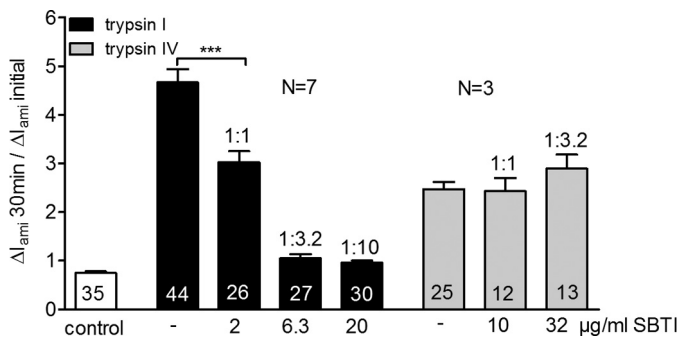


FIGURE 3. The polypeptide inhibitor SBTI prevents activation of ENaC by trypsin I but not trypsin IV. Oocytes expressing $\alpha\beta\gamma$ ENaC were incubated for 30 min in protease-free solution (control), in trypsin I (2 μ g/ml), in trypsin IV (10 μ g/ml), in trypsin I plus SBTI, or in trypsin IV plus SBTI. The ratio of protease to SBTI is indicated above the columns. Columns represent the relative effect of the incubation on ΔI_{ami} calculated as the ratio of ΔI_{ami} measured after 30-min incubation (ΔI_{ami} 30 min) to the initial ΔI_{ami} (ΔI_{ami} initial) measured before incubation. The numbers inside the columns indicate the number of individual oocytes measured. N indicates the number of different batches of oocytes. ***, $p < 0.001$, unpaired t test. Error bars, S.E.

proteolytic activation of ENaC by trypsin IV involves a critical cleavage site (Lys-189) in the extracellular domain of the γ -subunit.

Mutating Three Putative Trypsin Cleavage Sites (Lys-168, Lys-170, and Arg-172) in Addition to the Putative Proctasin, Plasmin, and Neutrophil Elastase Cleavage Sites of ENaC Prevents Trypsin I Activation of Human ENaC—Our finding that mutating Lys-189 in γ ENaC reduces proteolytic ENaC activation by trypsin IV but not by trypsin I indicates that different preferential cleavage sites exist for the two trypsins. Using the MEROPS database, we searched for putative trypsin I cleavage sites within the critical region of γ ENaC where the final channel activating cleavage event is thought to occur (Fig. 6) (8). We identified two lysine residues (Lys-168 and Lys-170) and one arginine residue (Arg-172) in γ ENaC that represent putative cleavage sites for trypsin I. In addition,

trypsin I may cleave γ ENaC at previously described putative cleavage sites for proctasin (RKRK¹⁷⁸), plasmin (Lys-189), and neutrophil elastase (Val-182 and Val-193). To investigate the importance of these sites for trypsin I-dependent activation of ENaC, we investigated the stimulatory effect of trypsin I on ΔI_{ami} in oocytes expressing wild-type $\alpha\beta\gamma$ ENaC or a mutant channel lacking the potential cleavage sites for trypsin I, proctasin, plasmin, and neutrophil elastase ($\alpha\beta\gamma_{K168A,K170A,R172A,RKRK178AAAA,V182G,V193G,K189A}$ ENaC). As shown in Fig. 7A, trypsin I failed to stimulate this mutant channel. Recently, we reported that mutating two phenylalanines (γ FF¹⁷⁴) in the vicinity of the putative proctasin cleavage site (Fig. 6) prevents proteolytic ENaC activation by chymotrypsin but not by trypsin I (8). In the present study, we confirmed these findings (Fig. 7A). Moreover, we demonstrated that chymotrypsin, unlike trypsin I, was able to activate at least in part the mutant channel ($\alpha\beta\gamma_{K168A,K170A,R172A,RKRK178AAAA,V182G,V193G,K189A}$ ENaC) lacking the potential cleavage sites for trypsin I, proctasin, plasmin, and neutrophil elastase (Fig. 7A). These findings indicate that trypsin I cleaves γ ENaC at sites that are distinct from the chymotrypsin sites.

Proteolytic activation of γ ENaC is associated with the appearance of γ ENaC cleavage products at the cell surface. To detect γ ENaC fragments at the cell surface, a biotinylation approach and an antibody that recognizes the intracellular carboxyl terminus of γ ENaC were used. The predominant γ ENaC fragment detected at the cell surface of untreated wild-type $\alpha\beta\gamma$ ENaC-expressing control oocytes had a molecular mass of ~ 76 kDa (Fig. 7B). This cleavage product results from cleavage of γ ENaC by endogenous proteases like furin at the so-called furin cleavage site, Arg-138 (8) (Fig. 7C). In untreated oocytes expressing the mutant channels $\alpha\beta\gamma_{FF174AA}$ ENaC or $\alpha\beta\gamma_{K168A,K170A,R172A,RKRK178AAAA,V182G,V193G,K189A}$ ENaC, the predominant γ ENaC fragment detected at the cell surface also had a molecular mass of ~ 76 kDa (Fig. 7B). In oocytes expressing wild-type ENaC, either protease, chymotrypsin or trypsin I, resulted in the disappearance of the ~ 76 kDa band and in the appearance of a ~ 67 kDa γ ENaC fragment (Fig. 7B, blot on the left). This ~ 67 -kDa fragment is likely to represent the pool of activated ENaC (8, 9, 13) resulting from the final activating cleavage event in the critical region of γ ENaC distal to the furin site (Fig. 7C). In oocytes expressing $\alpha\beta\gamma_{FF174AA}$ ENaC, chymotrypsin failed to generate the ~ 67 -kDa fragment, consistent with its failure to activate ENaC currents and consistent with our previous findings (8). In contrast, exposure of $\alpha\beta\gamma_{FF174AA}$ ENaC-expressing oocytes to trypsin I resulted in the appearance of the ~ 67 -kDa fragment, consistent with the observed current stimulation similar to that in oocytes expressing wild-type $\alpha\beta\gamma$ ENaC (Fig. 7, A and B, blot in the middle). These results indicate that proteolytic ENaC activation by trypsin I does not require the presence of the putative chymotrypsin sites (FF¹⁷⁴) (8).

In oocytes expressing $\alpha\beta\gamma_{K168A,K170A,R172A,RKRK178AAAA,V182G,V193G,K189A}$ ENaC, chymotrypsin partially converted the ~ 76 -kDa fragment to the ~ 67 -kDa form, consistent with its partial stimulatory effect on ENaC currents. As expected from the failure of trypsin I to activate ENaC currents in oocytes

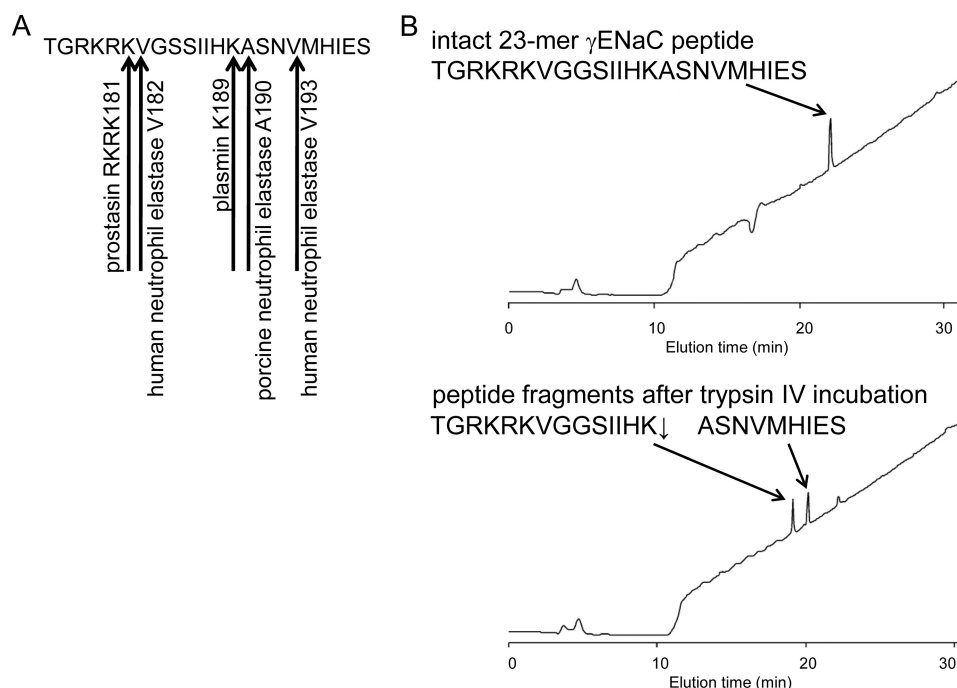


FIGURE 4. Trypsin IV cleaves within the extracellular domain of human γ ENaC. *A*, sequence of the 23-mer γ ENaC peptide showing putative cleavage sites for proteolytic ENaC activation. *B*, the 23-mer γ ENaC peptide (500 μ M) was incubated with trypsin IV (50 μ g/ml) for 30 min, and cleavage products were identified by HPLC and mass spectrometry.

expressing $\alpha\beta\gamma_{K168A,K170A,R172A,RKRK178AAAA,V182G,V193G,K189A}$ ENaC, trypsin I failed to shift the ~ 76 kDa band to a ~ 67 kDa band (Fig. 7, *B* and *C*, blot on the right). Taken together, these results demonstrate the inability of trypsin I to activate $\alpha\beta\gamma_{K168A,K170A,R172A,RKRK178AAAA,V182G,V193G,K189A}$ ENaC and the inability of chymotrypsin to activate $\alpha\beta\gamma_{FF174AA}$ ENaC.

Combined Mutation of the Putative Prostatic (RKRK¹⁷⁸), Plasmin (Lys-189), and Neutrophil Elastase (Val-182 and Val-193) Cleavage Sites or Combined Mutation of the Three Putative Trypsin I Cleavage Sites (Lys-168, Lys-170, and Arg-172) of Human γ ENaC Does Not Reduce the Stimulatory Effect of Trypsin I—Next, we investigated whether the combined mutation of the three predicted trypsin cleavage sites (Lys-168, Lys-170, and Arg-172) or the combined mutation of the putative cleavage sites for prostatic (RKRK¹⁷⁸), plasmin (Lys-189), and neutrophil elastase (Val-182 and Val-193) is sufficient to abolish ENaC activation by trypsin I. To do so, we generated two mutant channels, $\gamma_{K168A,K170A,R172A}$ ENaC and $\gamma_{RKRK178AAAA,V182G,V193G,K189A}$ ENaC, and expressed wild-type $\alpha\beta\gamma$ ENaC or the mutant channels in oocytes. The combined mutation of the putative prostatic, plasmin, and neutrophil elastase cleavage sites in γ ENaC did not alter channel activation by trypsin I (Fig. 8). Similarly, the combined mutation of the three predicted trypsin I cleavage sites (Lys-168, Lys-170, and Arg-172) did not reduce ENaC activation by trypsin I. However, the combination of all of these mutations ($\gamma_{K168A,K170A,R172A,RKRK178AAAA,V182G,V193G,K189A}$) prevented proteolytic activation of ENaC by trypsin I (Figs. 7 and 8). Hence, we identified functionally relevant cleavage sites in γ ENaC involved in proteolytic channel activation by trypsin I.

Effect of Mutating a Putative Trypsin IV Cleavage Site (Lys-189) in γ ENaC on the Concentration Dependence of the Stimulatory Effect of Trypsin IV and Trypsin I on ENaC Currents—We investigated the concentration dependence of the stimulatory effects of

trypsin I and trypsin IV on ENaC currents in oocytes expressing wild-type $\alpha\beta\gamma$ or $\alpha\beta\gamma_{K189A}$ ENaC (Fig. 9). As expected, trypsin I and trypsin IV increased ΔI_{ami} in a concentration-dependent manner. However, higher concentrations of trypsin IV were needed to achieve a similar degree of channel activation as with trypsin I. A possible explanation for this is that more functionally relevant cleavage sites exist in the critical region of γ ENaC for trypsin I than for trypsin IV. The concentration dependence of the stimulatory effect of trypsin I on wild-type ENaC was similar to that on the $\alpha\beta\gamma_{K189A}$ mutant channel. In contrast, for $\alpha\beta\gamma_{K189A}$ ENaC, the trypsin IV concentration-response curve was shifted to the right. These data are in good agreement with the results shown in Fig. 5 and confirm the functional relevance of the γ Lys-189 residue for proteolytic ENaC activation by trypsin IV but not by trypsin I.

Expression of Trypsinogen IV in Intact Human Kidney Tissue and in Cultured HPTCs—ENaC plays a major role in mediating sodium transport in the kidney. To investigate whether trypsinogen IV is also expressed in the human kidney, we performed RT-PCR experiments (Fig. 10). We assessed the expression of trypsinogen IV mRNA both in intact human kidney tissue and in human kidney tissue-derived short term cultures of proximal tubular epithelial cells (HPTCs) using RT-PCR. Both sources yielded PCR products of the expected size (474 bp) that, upon sequencing, were verified to represent human trypsinogen IV (Fig. 10). The identical PCR product was obtained from a human prostate cancer-derived epithelial cell line (PC3), shown previously to express trypsinogen IV (34). In addition, we amplified a PCR product from intact kidney tissue (Fig. 10, lower band, left-hand lane). This product yielded an oligonucleotide sequence that is unequivocally related to trypsin IV and may represent an as yet unde-

Trypsin IV Cleavage and Activation of ENaC

scribed splice variant of trypsin IV. “Negative controls” did not yield any bands.

Trypsin IV Stimulates ENaC in Human Airway Epithelial Cells (H441)—ENaC mediates sodium transport in the airway epithelium (39, 40), and human distal airway epithelial cells express trypsinogen IV (34). To investigate whether trypsin IV can stimulate ENaC-mediated transepithelial sodium transport

in distal airway epithelial cells, we measured I_{SC} in cultured H441 distal airway epithelial cells known to express ENaC (41, 42). Cells were pretreated with a furin/convertase inhibitor and SBTI to minimize constitutive ENaC activation by endogenous proteases (27, 29, 37). The furin/convertase inhibitor and SBTI remained present throughout the experiment. Apical application of trypsin IV (41 $\mu\text{g}/\text{ml}$), which is known to be resistant to SBTI, resulted in a pronounced increase in I_{SC} (Fig. 11A). In contrast, no I_{SC} stimulation was observed in matched vehicle-treated control cells (Fig. 11B). In cells treated with trypsin IV, subsequent application of amiloride (10 μM) to the apical side caused a larger I_{SC} decrease than in vehicle-treated control cells. Moreover, in the presence of amiloride application of trypsin IV failed to stimulate I_{SC} (Fig. 11B). Fig. 11C summarizes results from similar experiments as shown in Fig. 11, A and B. A stimulatory effect of trypsin IV on I_{SC} was observed in each experiment ($n = 4$) in which trypsin IV was tested (Fig. 11C). On average, apical application of trypsin IV stimulated ENaC-mediated I_{SC} by about 2.3-fold. Taken together, these findings indicate that the I_{SC} increase observed upon application of trypsin IV is caused by a stimulation of ENaC-mediated transepithelial sodium transport.

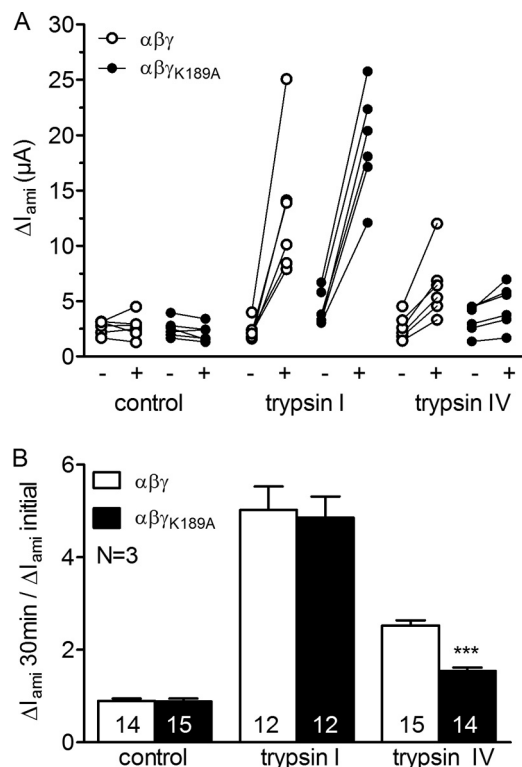


FIGURE 5. Mutation of γK189A suppresses ENaC activation by trypsin IV, not trypsin I. Oocytes expressing $\alpha\beta\gamma$ (open symbols) or $\alpha\beta\gamma_{K189A}$ ENaC (filled symbols) were incubated for 30 min in protease-free solution (control) or in a solution containing trypsin I (2 $\mu\text{g}/\text{ml}$) or trypsin IV (10 $\mu\text{g}/\text{ml}$). Amiloride-sensitive whole-cell currents (ΔI_{ami}) were determined before (–) and after (+) incubation. *A*, individual ΔI_{ami} values from a representative experiment using one batch of oocytes. Data points obtained from individual oocytes are connected by a line. *B*, summary of similar experiments as shown in *A*. Columns represent the relative effect of the incubation on ΔI_{ami} calculated as the ratio of ΔI_{ami} measured after 30-min incubation ($\Delta I_{ami} 30 \text{ min}$) to the initial ΔI_{ami} ($\Delta I_{ami} \text{ initial}$) measured before incubation. Numbers inside the columns indicate the number of individual oocytes measured. *N* indicates the number of different batches of oocytes. ***, $p < 0.001$, unpaired *t* test. Error bars, S.E.

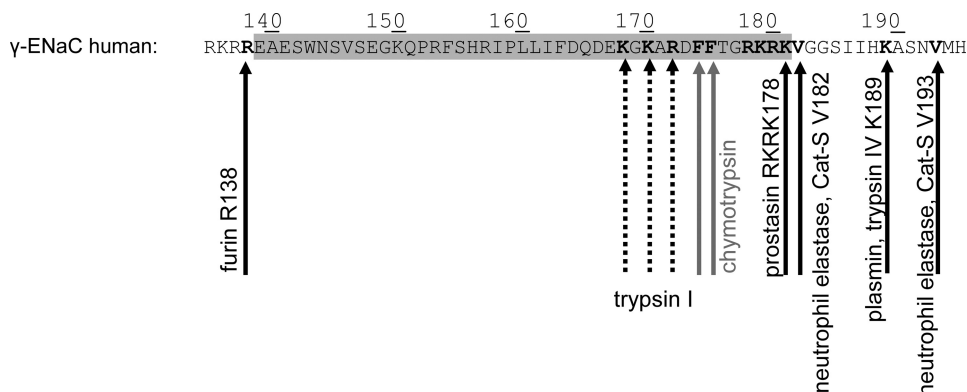


FIGURE 6. Sequence of human γ ENaC (amino acids 135–195). Amino acid sequence of human γ ENaC derived from the UniProt Database (UniProt number P51170). The putative cleavage sites for furin (Arg-138), trypsin I (Lys-168, Lys-170, and Arg-172), chymotrypsin (FF¹⁷⁴), prostatic (RKRK¹⁷⁸), human neutrophil elastase (Val-182 and Val-193), and plasmin (Lys-189) are indicated in boldface type and marked by arrows.

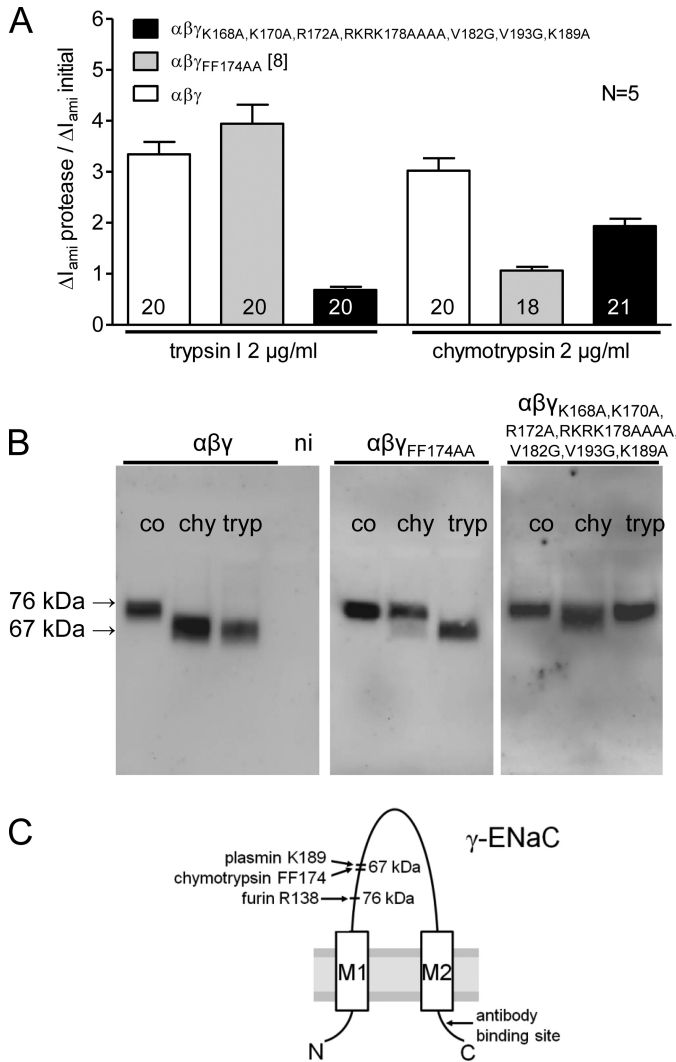


FIGURE 7. Mutating three putative trypsin I cleavage sites (Lys-168, Lys-170, and Arg-172) in addition to the putative prostatic, plasmin, and neutrophil elastase cleavage sites of ENaC prevents trypsin I activation of human ENaC. Continuous whole-cell current measurements were performed in oocytes expressing $\alpha\beta\gamma$, $\alpha\beta\gamma_{FF174AA}$, or $\alpha\beta\gamma_{K168A, K170A, R172A, RKRK178AAAA, V182G, V193G, K189A}$ ENaC. ΔI_{ami} was determined before and after superfusing the oocytes with chymotrypsin (2 μ g/ml) or trypsin I (2 μ g/ml) (A). For biotinylation experiments, matched oocytes were preincubated for 30 min in protease-free solution (control; co) or in a solution containing either chymotrypsin (chy; 2 μ g/ml) or trypsin I (tryp; 2 μ g/ml). In parallel experiments, expression of biotinylated γ ENaC at the cell surface was analyzed by SDS-PAGE and followed by Western blot (B). A, columns represent relative effects of trypsin I or chymotrypsin on ΔI_{ami} calculated as the ratio of ΔI_{ami} after trypsin I or chymotrypsin superfusion ($\Delta I_{ami} \text{ protease}$) to the initial ΔI_{ami} ($\Delta I_{ami} \text{ initial}$). The numbers inside the columns indicate the number of individual oocytes measured. N indicates the number of different batches of oocytes. B, representative Western blots from oocytes expressing $\alpha\beta\gamma$, $\alpha\beta\gamma_{FF174AA}$, or $\alpha\beta\gamma_{K168A, K170A, R172A, RKRK178AAAA, V182G, V193G, K189A}$ ENaC. γ ENaC was detected with an antibody against the carboxyl terminus of human γ ENaC. In non-injected oocytes (ni), γ ENaC-specific signals were absent (data not shown). C, model of the γ ENaC subunit showing cleavage sites for proteolytic activation and the binding site of the antibody used. Error bars, S.E.

study did not identify the isoform of trypsin present in the collecting ducts, it is likely that the antibody detects both trypsin I and trypsin IV, which differ only within the active site. Thus, trypsin IV may proteolytically activate ENaC expressed at the apical membrane of the renal collecting duct. We previously have shown that trypsin I can activate ENaC in microdissected mouse distal nephron tissue (14). Here, we have demonstrated

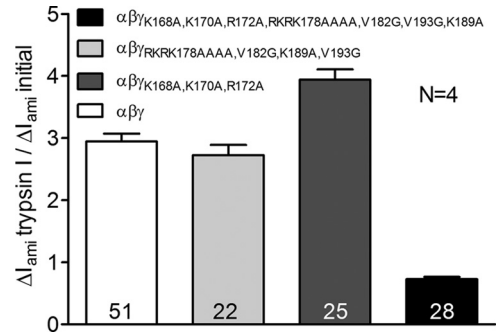


FIGURE 8. Combined mutation of the putative prostatic (RKRK¹⁷⁸), plasmin (Lys-189), and neutrophil elastase (Val-182 and Val-193) cleavage sites or combined mutation of the three putative trypsin I cleavage sites (Lys-168, Lys-170, and Arg-172) of human γ ENaC does not reduce the stimulatory effect of trypsin I. Continuous whole-cell current measurements were performed in oocytes expressing $\alpha\beta\gamma$, $\alpha\beta\gamma_{K168A, K170A, R172A}$, $\alpha\beta\gamma_{RK178AAAA, V182G, V193G, K189A}$, or $\alpha\beta\gamma_{K168A, K170A, R172A, RKRK178AAAA, V182G, V193G, K189A}$ ENaC. ΔI_{ami} was determined before and after superfusing the oocytes with trypsin I (2 μ g/ml). The columns represent the relative effect of trypsin I on ΔI_{ami} calculated as the ratio of ΔI_{ami} after trypsin I superfusion ($\Delta I_{ami} \text{ trypsin I}$) to the initial ΔI_{ami} ($\Delta I_{ami} \text{ initial}$). The numbers inside the columns indicate the number of individual oocytes measured. N indicates the number of different batches of oocytes. Error bars, S.E.

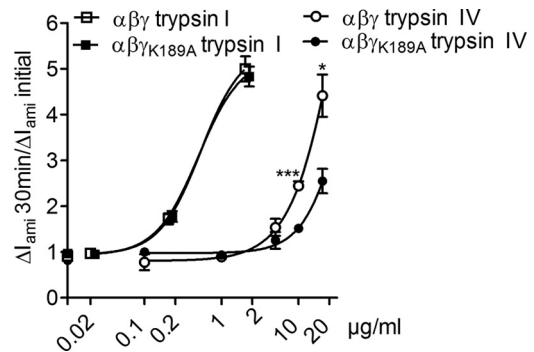


FIGURE 9. Effect of mutating a putative trypsin IV cleavage site (Lys-189) in γ ENaC on the concentration dependence of the stimulatory effect of trypsin IV and trypsin I on ENaC currents. Average concentration-response curves determined from experiments, as shown in Fig. 5. Oocytes expressing $\alpha\beta\gamma$ (open symbols) or $\alpha\beta\gamma_{K189A}$ ENaC (filled symbols) were incubated for 30 min in solutions containing different concentrations of trypsin I or trypsin IV. Amiloride-sensitive whole-cell currents (ΔI_{ami}) were determined before ($\Delta I_{ami} \text{ initial}$) and after incubation ($\Delta I_{ami} \text{ 30 min}$). Each data point represents the average relative stimulatory effect of trypsin IV or trypsin I on ΔI_{ami} with 4–46 oocytes measured. Data were fitted using a sigmoidal dose response (variable slope). *, $p < 0.05$; ***, $p < 0.001$, unpaired t test. Error bars, S.E.

the expression of trypsinogen IV mRNA in human proximal tubular epithelial cells. These data support the concept that trypsinogen IV/trypsin IV release from proximal tubule cells into the tubular lumen could result in a downstream activation of ENaC in the distal tubule and therefore may play a role in ENaC regulation *in vivo*.

A single amino acid substitution within the active site region (glycine 198 to arginine, trypsin I to trypsin IV) dramatically alters the substrate specificity and inhibitor resistance of the two enzymes. Trypsin IV is resistant to polypeptide trypsin inhibitors, such as SBTI (18). Moreover, trypsin IV can degrade and inactivate these trypsin inhibitors (19, 34, 43–45). In contrast to trypsin I, trypsin IV resists autoactivation and autolysis (43). Thus, once generated, trypsin IV may retain activity for prolonged periods, which could enhance its capacity to regulate multiple cell types. In addition to other proteases, including

Trypsin IV Cleavage and Activation of ENaC

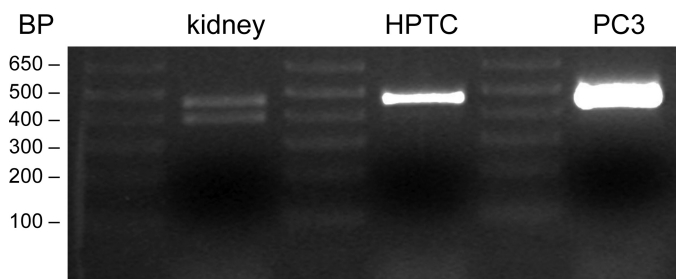


FIGURE 10. Expression of trypsinogen IV in human intact whole kidney and in HPTCs. PCR products for reverse-transcribed mRNA isolated from intact human kidney (*left*), from cultured HPTCs (*middle*), or from prostate cancer-derived human epithelial cells (PC3) (*right*) were obtained using the PCR primers and procedures outlined under "Experimental Procedures." The sizes of the PCR products can be estimated from the base pair (BP) ladder standards shown.

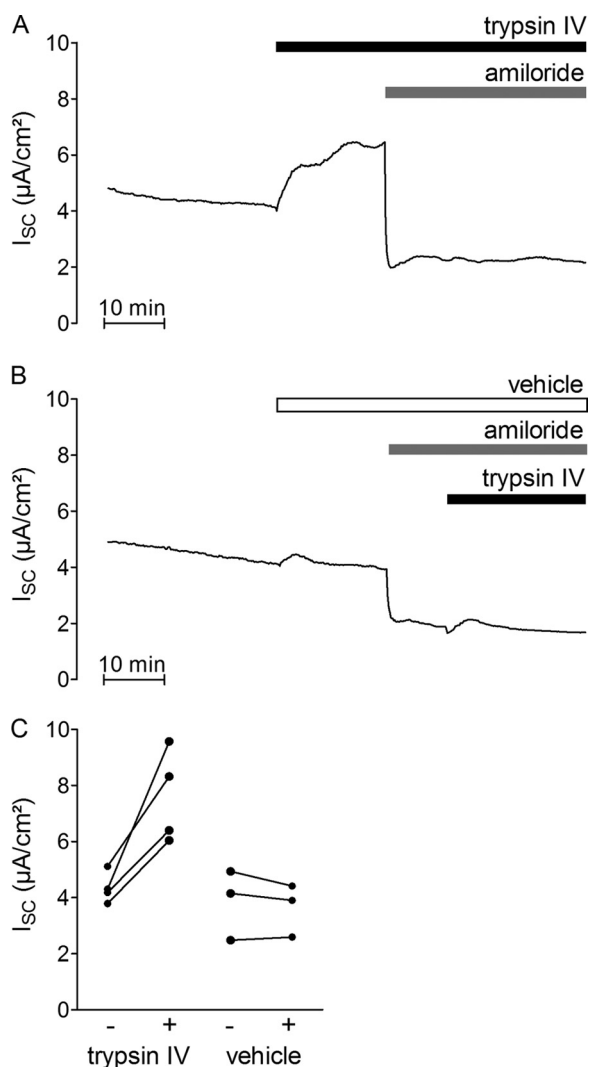


FIGURE 11. Trypsin IV stimulates ENaC in human airway epithelial cells (H441). A and B, representative equivalent short circuit current (I_{sc}) recordings from H441 distal airway epithelial cells. Trypsin IV (41 $\mu\text{g/ml}$) (A) or vehicle (0.9% NaCl) (B) was added to the apical bath solution of H441 cells as indicated by the horizontal bars. Amiloride (10 μM) was added apically to confirm that the stimulated I_{sc} was mediated by ENaC. C, summary of results from similar experiments as shown in A and B. Data points represent individual I_{sc} values obtained before and after (connected by a line) treatment with trypsin IV or vehicle.

neutrophil elastase and cathepsin-S, trypsin IV is up-regulated during inflammation and in tumors (22). Recent reports implicate trypsin IV in prostate cancer metastasis (25, 26). Trypsin IV may be a biomarker that is prognostic of future metastasis and therefore survival in prostate cancer and non-small cell lung cancer (25, 46). The up-regulation of trypsin IV is accompanied by an increased probability of metastatic progression of the disease (26). Importantly, metastatic invasion of prostate cancer was reduced by inhibition or gene silencing of trypsin IV in cell culture and in an orthotopic mouse model of prostate cancer (25). Therefore, it is of considerable interest to understand the actions of trypsin IV and related proteases. Our results show that trypsin IV, like trypsin I, activates ENaC but that these closely related proteases do so by cleaving γ ENaC at distinct sites. Our findings identify an additional mechanism by which trypsin IV can regulate cells. We have previously shown that trypsin IV can also regulate cells by cleaving protease-activated receptors 1 and 2 to regulate inflammation and pain (34).

We observed that trypsin IV, applied to the apical membrane, activates ENaC in human airway epithelial cells. Airway epithelial cells have been shown to express trypsinogen IV (34), raising the possibility that trypsin IV could activate ENaC in epithelial cells in an autocrine manner. Trypsinogen IV is co-expressed with ENaC in other epithelial cell lines. The human colonic epithelial cell lines CaCo-2 and HT-29 co-express trypsinogen IV and ENaC (28, 34, 42, 47). The co-expression of ENaC and trypsinogen IV in colonic epithelial cells supports the concept that local trypsinogen IV release in the colon may contribute to ENaC function in the colon *in vivo*. Due to its inhibitor resistance, trypsin IV may remain active for prolonged periods in the colonic lumen and therefore may play a role in the regulation of ENaC in different tissues. Recent reports suggest that ENaC is important for sodium and electrolyte balance in the intestine and that its down-regulation could contribute to the pathogenesis of diarrhea in Crohn disease (28). Hence, activation of ENaC by secreted trypsin IV in epithelial cells of the colon may limit fluid loss induced by decreased expression of ENaC in Crohn disease. Further studies are required to examine this possibility and to define the mechanisms that regulate the secretion and activation of trypsinogen IV in epithelial tissues.

In summary, we show, for the first time, that trypsin IV can activate ENaC by proteolytic cleavage at a site that is distinct from the sites cleaved by trypsin I. Based on our findings, we suggest that trypsin IV may contribute to ENaC regulation in several epithelial tissues co-expressing ENaC and trypsin IV, such as in the kidney and in the lung. Moreover, we have identified the functionally relevant trypsin cleavage sites in the γ -subunit of human ENaC. We report that trypsin IV preferentially cleaves at γ Lys-189 and therefore shows a more specific cleavage pattern than trypsin I, which cleaves ENaC at multiple sites. The availability of multiple cleavage sites for trypsin I may explain why the concentration of trypsin I needed for channel activation is lower than that of trypsin IV. Our results support the concept that the critical second cleavage event in γ ENaC, which represents the final step in proteolytic ENaC activation, may occur at different sites within a defined region of the γ -sub-

unit. The availability of several cleavage sites in this region with preferences for different types of proteases may provide a basis for tissue-specific proteolytic ENaC activation under physiological and pathophysiological conditions.

Acknowledgments—The expert technical assistance of Céline Grüninger, Christina Lang, Sonja Mayer, and Ralf Rinke is gratefully acknowledged.

REFERENCES

1. Garty, H., and Palmer, L. G. (1997) Epithelial sodium channels: function, structure, and regulation. *Physiol. Rev.* **77**, 359–396
2. Kellenberger, S., and Schild, L. (2002) Epithelial sodium channel/degenerin family of ion channels: a variety of functions for a shared structure. *Physiol. Rev.* **82**, 735–767
3. Jasti, J., Furukawa, H., Gonzales, E. B., and Gouaux, E. (2007) Structure of acid-sensing ion channel 1 at 1.9 Å resolution and low pH. *Nature* **449**, 316–323
4. Stockand, J. D., Staruschenko, A., Pochynyuk, O., Booth, R. E., and Silverthorn, D. U. (2008) Insight toward epithelial Na⁺ channel mechanism revealed by the acid-sensing ion channel 1 structure. *IUBMB Life* **60**, 620–628
5. Stewart, A. P., Haerteis, S., Diakov, A., Korbmacher, C., and Edwardson, J. M. (2011) Atomic force microscopy reveals the architecture of the epithelial sodium channel (ENaC). *J. Biol. Chem.* **286**, 31944–31952
6. Kleyman, T. R., Carattino, M. D., and Hughey, R. P. (2009) ENaC at the cutting edge: regulation of epithelial sodium channels by proteases. *J. Biol. Chem.* **284**, 20447–20451
7. Rossier, B. C., and Stutts, M. J. (2009) Activation of the epithelial sodium channel (ENaC) by serine proteases. *Annu. Rev. Physiol.* **71**, 361–379
8. Haerteis, S., Krappitz, M., Diakov, A., Krappitz, A., Rauh, R., and Korbmacher, C. (2012) Plasmin and chymotrypsin have distinct preferences for channel activating cleavage sites in the γ -subunit of the human epithelial sodium channel. *J. Gen. Physiol.* **140**, 375–389
9. Bruns, J. B., Carattino, M. D., Sheng, S., Maarouf, A. B., Weisz, O. A., Pilewski, J. M., Hughey, R. P., and Kleyman, T. R. (2007) Epithelial Na⁺ channels are fully activated by furin- and prostaticin-dependent release of an inhibitory peptide from the γ subunit. *J. Biol. Chem.* **282**, 6153–6160
10. Passero, C. J., Mueller, G. M., Rondon-Berrios, H., Tofovic, S. P., Hughey, R. P., and Kleyman, T. R. (2008) Plasmin activates epithelial Na⁺ channels by cleaving the γ subunit. *J. Biol. Chem.* **283**, 36586–36591
11. Adebamiro, A., Cheng, Y., Rao, U. S., Danahay, H., and Bridges, R. J. (2007) A segment of γ ENaC mediates elastase activation of Na⁺ transport. *J. Gen. Physiol.* **130**, 611–629
12. Patel, A. B., Chao, J., and Palmer, L. G. (2012) Tissue kallikrein activation of the epithelial Na channel. *Am. J. Physiol. Renal Physiol.* **303**, F540–F550
13. Diakov, A., Bera, K., Mokrushina, M., Krueger, B., and Korbmacher, C. (2008) Cleavage in the γ -subunit of the epithelial sodium channel (ENaC) plays an important role in the proteolytic activation of near-silent channels. *J. Physiol.* **586**, 4587–4608
14. Nesterov, V., Dahlmann, A., Bertog, M., and Korbmacher, C. (2008) Trypsin can activate the epithelial sodium channel (ENaC) in microdissected mouse distal nephron. *Am. J. Physiol. Renal Physiol.* **295**, F1052–F1062
15. Koshikawa, N., Hasegawa, S., Nagashima, Y., Mitsuhashi, K., Tsubota, Y., Miyata, S., Miyagi, Y., Yasumitsu, H., and Miyazaki, K. (1998) Expression of trypsin by epithelial cells of various tissues, leukocytes, and neurons in human and mouse. *Am. J. Pathol.* **153**, 937–944
16. Navarrete, M., Ho, J., Krokhn, O., Ezzati, P., Rigatto, C., Reslerova, M., Rush, D. N., Nickerson, P., and Wilkins, J. A. (2013) Proteomic characterization of serine hydrolase activity and composition in normal urine. *Clin. Proteomics* **10**, 17
17. Emi, M., Nakamura, Y., Ogawa, M., Yamamoto, T., Nishide, T., Mori, T., and Matsubara, K. (1986) Cloning, characterization and nucleotide sequences of two cDNAs encoding human pancreatic trypsinogens. *Gene* **41**, 305–310

18. Wiegand, U., Corbach, S., Minn, A., Kang, J., and Müller-Hill, B. (1993) Cloning of the cDNA encoding human brain trypsinogen and characterization of its product. *Gene* **136**, 167–175
19. Nyaruhucha, C. N., Kito, M., and Fukuoaka, S. I. (1997) Identification and expression of the cDNA-encoding human mesotrypsin(ogen), an isoform of trypsin with inhibitor resistance. *J. Biol. Chem.* **272**, 10573–10578
20. Gallatz, K., Medveczky, P., Németh, P., Szilágyi, L., Gráf, L., and Palkovits, M. (2007) Human trypsin(ogen) 4-like immunoreactivity in the white matter of the cerebral cortex and the spinal cord. *Ideggogyaszati szemle* **60**, 118–123
21. Tóth, J., Siklódi, E., Medveczky, P., Gallatz, K., Németh, P., Szilágyi, L., Gráf, L., and Palkovits, M. (2007) Regional distribution of human trypsinogen 4 in human brain at mRNA and protein level. *Neurochem. Res.* **32**, 1423–1433
22. Knecht, W., Cottrell, G. S., Amadesi, S., Mohlin, J., Skåregårde, A., Gedda, K., Peterson, A., Chapman, K., Hollenberg, M. D., Vergnolle, N., and Bunnett, N. W. (2007) Trypsin IV or mesotrypsin and p23 cleave protease-activated receptors 1 and 2 to induce inflammation and hyperalgesia. *J. Biol. Chem.* **282**, 26089–26100
23. Ceppa, E. P., Lyo, V., Grady, E. F., Knecht, W., Grahn, S., Peterson, A., Bunnett, N. W., Kirkwood, K. S., and Cattaruzza, F. (2011) Serine proteases mediate inflammatory pain in acute pancreatitis. *Am. J. Physiol. Gastrointest. Liver Physiol.* **300**, G1033–G1042
24. Cattaruzza, F., Amadesi, S., Carlsson, J. F., Murphy, J. E., Lyo, V., Kirkwood, K., Cottrell, G. S., Bogyo, M., Knecht, W., and Bunnett, N. W. (2014) Serine proteases and protease-activated receptor 2 mediate the proinflammatory and algescic actions of diverse stimulants. *Br. J. Pharmacol.* **10.1111/bph.12738**
25. Hockla, A., Miller, E., Salameh, M. A., Copland, J. A., Radisky, D. C., and Radisky, E. S. (2012) PRSS3/mesotrypsin is a therapeutic target for metastatic prostate cancer. *Mol. Cancer Res.* **10**, 1555–1566
26. Radisky, E. S. (2013) PRSS3/mesotrypsin in prostate cancer progression: implications for translational medicine. *Asian J. Androl.* **15**, 439–440
27. Svenningsen, P., Bistrup, C., Friis, U. G., Bertog, M., Haerteis, S., Krueger, B., Stubbe, J., Jensen, O. N., Thiesson, H. C., Uhrenholt, T. R., Jespersen, B., Jensen, B. L., Korbmacher, C., and Skøtt, O. (2009) Plasmin in nephrotic urine activates the epithelial sodium channel. *J. Am. Soc. Nephrol.* **20**, 299–310
28. Zeissig, S., Bergann, T., Fromm, A., Bojarski, C., Heller, F., Guenther, U., Zeitz, M., Fromm, M., and Schulzke, J. D. (2008) Altered ENaC expression leads to impaired sodium absorption in the noninflamed intestine in Crohn's disease. *Gastroenterology* **134**, 1436–1447
29. Haerteis, S., Krappitz, M., Bertog, M., Krappitz, A., Baraznenok, V., Henderson, I., Lindström, E., Murphy, J. E., Bunnett, N. W., and Korbmacher, C. (2012) Proteolytic activation of the epithelial sodium channel (ENaC) by the cysteine protease cathepsin-S. *Pflügers Arch.* **464**, 353–365
30. Haerteis, S., Krueger, B., Korbmacher, C., and Rauh, R. (2009) The δ -subunit of the epithelial sodium channel (ENaC) enhances channel activity and alters proteolytic ENaC activation. *J. Biol. Chem.* **284**, 29024–29040
31. Rauh, R., Diakov, A., Tzschoppe, A., Korbmacher, J., Azad, A. K., Cuppens, H., Cassiman, J. J., Dötsch, J., Sticht, H., and Korbmacher, C. (2010) A mutation of the epithelial sodium channel associated with atypical cystic fibrosis increases channel open probability and reduces Na⁺ self inhibition. *J. Physiol.* **588**, 1211–1225
32. Krueger, B., Schlötzer-Schrehardt, U., Haerteis, S., Zenkel, M., Chankiewitz, V. E., Amann, K. U., Kruse, F. E., and Korbmacher, C. (2012) Four subunits ($\alpha\beta\gamma\delta$) of the epithelial sodium channel (ENaC) are expressed in the human eye in various locations. *Invest. Ophthalmol. Vis. Sci.* **53**, 596–604
33. Chung, H., Ramachandran, R., Hollenberg, M. D., and Muruve, D. A. (2013) Proteinase-activated receptor-2 transactivation of epidermal growth factor receptor and transforming growth factor- β receptor signaling pathways contributes to renal fibrosis. *J. Biol. Chem.* **288**, 37319–37331
34. Cottrell, G. S., Amadesi, S., Grady, E. F., and Bunnett, N. W. (2004) Trypsin IV, a novel agonist of protease-activated receptors 2 and 4. *J. Biol. Chem.* **279**, 13532–13539
35. Woolthead, A. M., Scott, J. W., Hardie, D. G., and Baines, D. L. (2005) Phenformin and 5-aminoimidazole-4-carboxamide-1- β -D-ribofuran-

Trypsin IV Cleavage and Activation of ENaC

- side (AICAR) activation of AMP-activated protein kinase inhibits transepithelial Na^+ transport across H441 lung cells. *J. Physiol.* **566**, 781–792
36. Bertog, M., Letz, B., Kong, W., Steinhoff, M., Higgins, M. A., Bielfeld-Ackermann, A., Frömter, E., Bunnett, N. W., and Korbmacher, C. (1999) Basolateral proteinase-activated receptor (PAR-2) induces chloride secretion in M-1 mouse renal cortical collecting duct cells. *J. Physiol.* **521**, 3–17
37. Tan, C. D., Selvanathar, I. A., and Baines, D. L. (2011) Cleavage of endogenous γ ENaC and elevated abundance of α ENaC are associated with increased Na^+ transport in response to apical fluid volume expansion in human H441 airway epithelial cells. *Pflügers Arch.* **462**, 431–441
38. Volk, T., Konstas, A. A., Bassalá, P., Ehmke, H., and Korbmacher, C. (2004) Extracellular Na^+ removal attenuates rundown of the epithelial Na^+ -channel (ENaC) by reducing the rate of channel retrieval. *Pflügers Arch.* **447**, 884–894
39. Eaton, D. C., Helms, M. N., Koval, M., Bao, H. F., and Jain, L. (2009) The contribution of epithelial sodium channels to alveolar function in health and disease. *Annu. Rev. Physiol.* **71**, 403–423
40. Hummler, E., and Planès, C. (2010) Importance of ENaC-mediated sodium transport in alveolar fluid clearance using genetically-engineered mice. *Cell Physiol. Biochem.* **25**, 63–70
41. Lazrak, A., and Matalon, S. (2003) cAMP-induced changes of apical membrane potentials of confluent H441 monolayers. *Am. J. Physiol. Lung Cell Mol. Physiol.* **285**, L443–L450
42. Ji, H. L., Su, X. F., Kedar, S., Li, J., Barbry, P., Smith, P. R., Matalon, S., and Benos, D. J. (2006) δ -Subunit confers novel biophysical features to $\alpha\beta\gamma$ -human ENaC via a physical interaction. *J. Biol. Chem.* **281**, 8233–8241
43. Szmola, R., Kukor, Z., and Sahin-Tóth, M. (2003) Human mesotrypsin is a unique digestive protease specialized for the degradation of trypsin inhibitors. *J. Biol. Chem.* **278**, 48580–48589
44. Sahin-Tóth, M. (2005) Human mesotrypsin defies natural trypsin inhibitors: from passive resistance to active destruction. *Protein Pept. Lett.* **12**, 457–464
45. Chen, J. M., Radisky, E. S., and Ferec, C. (2012) Human trypsins. in *Handbook of Proteolytic Enzymes* (Rawlings, N. D., and Salvesen, G. S., eds) pp. 2600–2609, Elsevier, Amsterdam
46. Diederichs, S., Bulk, E., Steffen, B., Ji, P., Tickenbrock, L., Lang, K., Zänker, K. S., Metzger, R., Schneider, P. M., Gerke, V., Thomas, M., Berdel, W. E., Serve, H., and Müller-Tidow, C. (2004) S100 family members and trypsinogens are predictors of distant metastasis and survival in early-stage non-small cell lung cancer. *Cancer Res.* **64**, 5564–5569
47. Ghilardi, C., Chiorino, G., Dossi, R., Nagy, Z., Giavazzi, R., and Bani, M. (2008) Identification of novel vascular markers through gene expression profiling of tumor-derived endothelium. *BMC Genomics* **9**, 201